ADVANCED FUNCTIONAL MATERIALS
www.afm-journal.de

Materials Views
www.MaterialsViews.com

A Controllable Synthesis of Rich Nitrogen-Doped Ordered Mesoporous Carbon for CO_2 Capture and Supercapacitors

Jing Wei, Dandan Zhou, Zhenkun Sun, Yonghui Deng, Yongyao Xia, and Dongyuan Zhao**

A controllable one-pot method to synthesize N-doped ordered mesoporous carbons (NMC) with a high N content by using dicyandiamide as a nitrogen source via an evaporation-induced self-assembly process is reported. In this synthesis, resol molecules can bridge the Pluronic F127 template and dicyandiamide via hydrogen bonding and electrostatic interactions. During thermosetting at 100 °C for formation of rigid phenolic resin and subsequent pyrolysis at 600 °C for carbonization, dicyandiamide provides closed N species while resol can form a stable framework, thus ensuring the successful synthesis of ordered N-doped mesoporous carbon. The obtained N-doped ordered mesoporous carbons possess tunable mesostructures (*p6m* and *Im$\bar{3}$m* symmetry) and pore size (3.1–17.6 nm), high surface area (494–586 $m^2\ g^{-1}$), and high N content (up to 13.1 wt%). Ascribed to the unique feature of large surface area and high N contents, NMC materials show high CO_2 capture of 2.8–3.2 mmol g^{-1} at 298 K and 1.0 bar, and exhibit good performance as the supercapacitor electrode with specific capacitances of 262 F g^{-1} (in 1 M H_2SO_4) and 227 F g^{-1} (in 6 M KOH) at a current density of 0.2 A g^{-1}.

1. Introduction

Ordered mesoporous carbons have received considerable attention owing to their large surface area, tunable pore structure, uniform and adjustable pore size, chemically inert nature, mechanical stability, and good conductivity. These outstanding features make them ideal candidates for applications in adsorption and separation, catalysis, electrochemistry, and sensors.[1] However, most of the mesoporous carbons have highly hydrophobic surface and a limited number of specific active sites, which impedes their practical application. It has been demonstrated that the incorporation of heteroatoms, such as boron, nitrogen, and oxygen, into the carbon lattice can significantly enhance the mechanical, semiconducting, field-emission, and electrical properties of carbon materials.[2] As a result, increasing efforts have been recently devoted to the synthesis of element-doped mesoporous carbons which combine the high mesoporosity and unique properties of doped carbon frameworks. Among them, nitrogen doping can enhance the surface polarity, electric conductivity, and electron-donor tendency of the mesoporous carbons, which enables their application in CO_2 capture, electric double-layer capacitors, fuel cells, and catalysis.[3]

N-doped mesoporous carbons (NMCs) are usually synthesized via the nanocasting approach, in which nitrogen-containing polymers as carbon and nitrogen sources are introduced into the pores of the ordered mesoporous silicas (i.e., the hard templates) by impregnation, followed by in situ carbonization and removal of the silica template.[4] This hard-templating synthesis method is time-consuming, costly, and unsuitable for mass production. Therefore, development of a reliable and facile strategy to synthesize N-doped mesoporous carbon without the use of a hard template is highly desirable. Recently, the organic-organic self-assembly of amphiphilic block copolymers poly(ethylene oxide)-*block*-poly(propylene oxide)-*block*-poly(ethylene oxide) (PEO-PPO-PEO) and phenolic resin (the carbon precursor) has proven to be a versatile route to synthesize ordered mesoporous carbons,[5] even at large scale.[6] Based on this method, some N-containing precursors, including melamine resins, urea-phenol-formaldehyde resin and dicyandiamide have been used as carbon sources to produce N-doped mesoporous carbons. Unfortunately, all these attempts only result in inferior pore structure with poor thermal stability or low N content.[7] The main reason is that the presence of Pluronic surfactant with high oxygen content can promote the decomposition of N-containing precursor, leading to collapsed mesostructures. In addition, the pyrolysis at high temperature can also accelerate the decomposition of N-containing frameworks, resulting in a low N content or collapsed mesostructure. Hao et al. reported the direct self-assembly of poly(benzoxazine-*co*-resol) followed by a carbonization process, obtaining N-doped porous carbons with well-defined hierachical porosities;[8] however, the N content was as low as 3.38 wt%. Recently, the facile synthesis of N-doped mesoporous carbon via the direct carbonization of ionic liquids with N-containing groups has also been reported; however, the mesoporous carbons prepared from direct carbonization methods have usually shown wide pore size and disordered mesostructure.[9] Direct synthesis of ordered mesoporous carbons with high N content and large surface area from organic–organic self-assembly still remains a great challenge.

J. Wei, D. D. Zhou, Z. K. Sun, Prof. Y. H. Deng, Prof. Y. Y. Xia, Prof. D. Y. Zhao
Department of Chemistry
Advanced Materials Laboratory
and State Key Laboratory of Molecular Engineering of Polymers
Fudan University
Shanghai 200433, P. R. China
E-mail: yhdeng@fudan.edu.cn; dyzhao@fudan.edu.cn

DOI: 10.1002/adfm.201202764

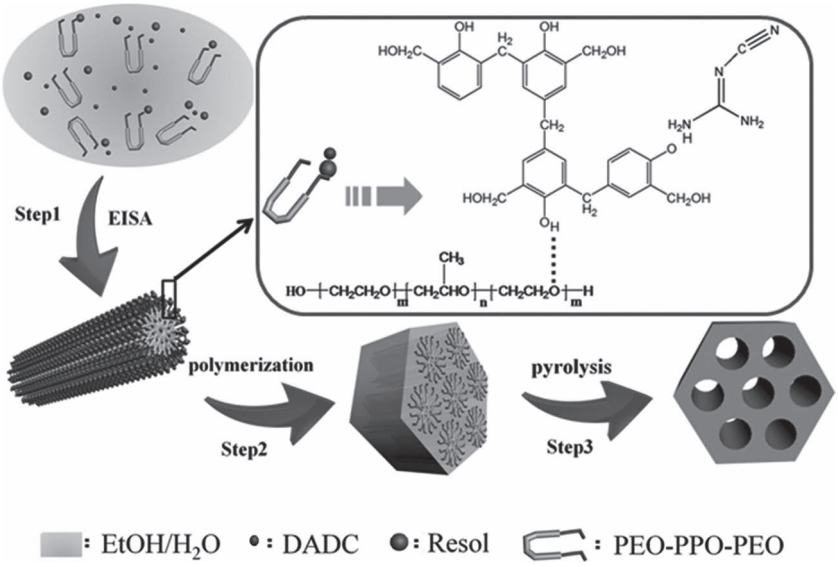

Scheme 1. The formation process of ordered N-doped mesoporous carbon from a one-pot assembly method using dicyandiamide (DCDA) as a nitrogen source.

Resol as a carbon source has unique properties, as follows.[5c] It has a moderate size and molecular weight (ca. 500 g mol^{-1}), which endows a good mobility for assembly. Secondly, it has multiple phenolic hydroxyl groups that can associate with the ethylene oxide (EO) repeating units in the PEO-containing block copolymer templates through hydrogen bonding and further co-assemble into ordered mesostructures with various symmetries. Thirdly, upon heating, resols can be polymerized into thermosetting phenolic resin that is thermally and chemically stable, and can be pyrolyzed into rigid carbon in inert atmosphere. However, resol does not contain nitrogen element. Dicyandiamide (DCDA), possessing one nitrile group and two amine groups, has high nitrogen content (66.7%) and can be converted to graphitic carbon nitride (g-C_3N_4) at high temperature (ca. 550 °C). Direct assembly of DCDA and Pluronic PEO-PPO-PEO copolymers leads to porous carbon nitrides with high N content but poor mesostructure and low surface area, due to the weak interaction between DCDA and PEO-PPO-PEO and the collapse of the framework during the pyrolysis for the removal of templates.[7c]

Herein, we report a one-pot controllable method to synthesize N-doped ordered mesoporous carbons with a high N content by using a low-molecular-weight soluble resol and DCDA as the carbon and nitrogen source, respectively, commercially available F127 as a soft template, and ethanol and water as a mixed solvent via evaporation-induced self-assembly (EISA) process. In this synthesis, resol molecules can bridge the Pluronic F127 template and DCDA via hydrogen bonding and electrostatic interactions during EISA process (**Scheme 1**). During thermosetting at 100 °C for formation of rigid phenolic resin and subsequent pyrolysis at 600 °C in N_2 for carbonization, DCDA provides closed N species while resol can form a stable framework, thus ensuring the successful synthesis of ordered NMCs. The obtained NMCs possess tunable mesostructures ($p6m$ and $Im\bar{3}m$ symmetry) and pore size (3.1–17.6 nm), high surface area (494–586 m^2 g^{-1}), and high N content (up to 13.1 wt%) by simply changing the amounts of F127, resol, and DCDA. The high nitrogen content is attributed to the introduction of DCDA, which can form stable microdomains of carbon nitrides in the matrix of phenolic resin. The rigid phenolic resin framework prevents the mesostructure from collapse during the removal of templates and carbonization, resulting in high surface area. Ascribed to the unique feature of large surface area and high N content, NMC materials show high CO_2 capture of 2.8–3.2 mmol g^{-1} at 298 K and 1.0 bar, and exhibit good performance as supercapacitor electrodes, with specific capacitances of 262 F g^{-1} (in 1 M H_2SO_4) and 227 F g^{-1} (in 6 M KOH) at a current density of 0.2 A g^{-1}.

2. Results and Discussion

By fixing the mass ratio of resol to F127 at 1:1 and varying the mass ratio of DCDA to resol, a series of samples was synthesized; these are denoted as H-NMC-x, where x is the mass ratio of DCDA to resol. Small-angle X-ray scattering (SAXS) pattern of the sample H-NMC-0 without addition of DCDA shows two resolved scattering peaks, which are indexed as the 10 and 11 planes of a 2D hexagonal mesostructure, i.e., the space group $p6m$ (**Figure 1**a), consistent with FDU-15 mesoporous carbons.[5c] Similar to H-NMC-0,

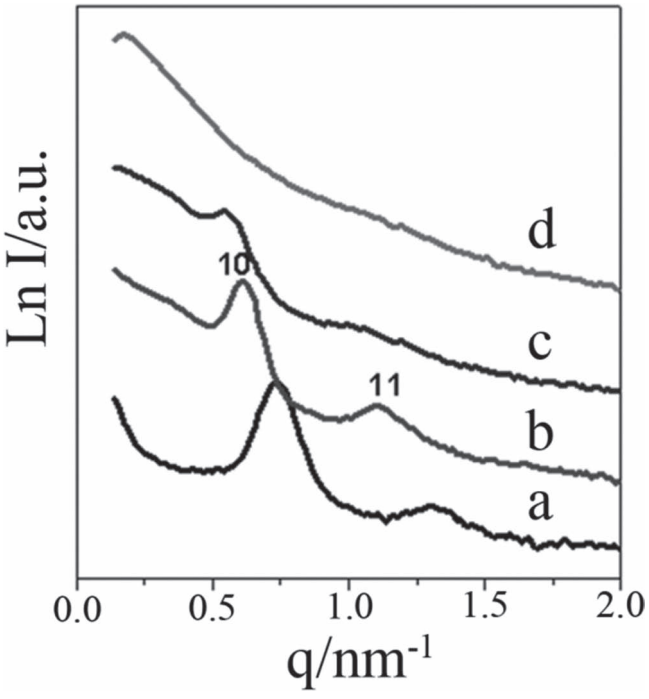

Figure 1. SAXS patterns of 2D hexagonal N-doped mesoporous carbon with different mass ratios of DCDA to resol: a) H-NMC-0; b) H-NMC-1.0; c) H-NMC-1.5; and d) H-NMC-2.5.

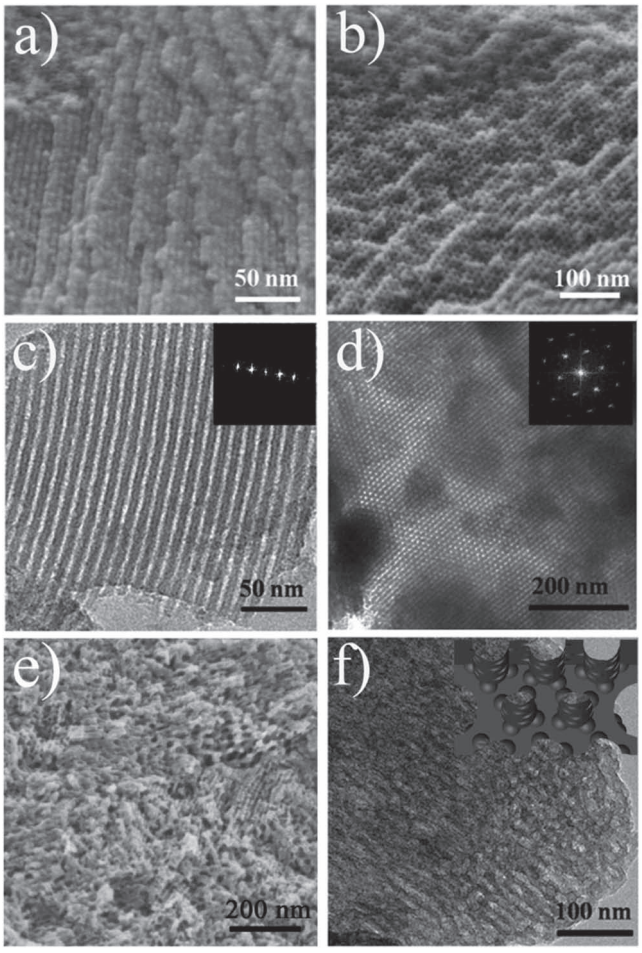

Figure 2. FESEM images (a,b) and TEM images (c,d) of the N-doped mesoporous carbons prepared from one-pot assembly method by using dicyandiamide as a precursor with mass ratio of 1.5 (DCDA/resol) (H-NMC-1.5). The insets in (c) and (d) are the corresponding FFT diffractograms. FESEM image (e) and TEM image (f) of the N-doped mesoporous carbon with mass ratio of 2.5 (DCDA/resol) (H-NMC-2.5); the inset in (f) is the corresponding structural model.

H-NMC-1.0 and -1.5 with different N contents show resolved SAXS patterns of *p6m* hexagonal mesostructure (Figure 1b,c). The slight decrease in the scattering intensity in the samples with a high amount of DCDA indicates that the ordered mesostructures are slightly degenerated. The unit cell parameters calculated from SAXS results are 9.8, 11.9, and 13.4 nm for the H-NMC-0, -1.0, and -1.5 samples, respectively, indicating that higher amounts of DCDA can dramatically cause the expansion of mesostructures. When the mass ratio of DCDA to resol was further increased to 2.5, the obtained H-NMC-2.5 sample shows no obvious scattering peak, which suggests that the co-assembly process is slightly hampered by excess DCDA (Figure 1d).

Field-emission scanning electron microscopy (FESEM) images of the representative H-NMC-1.5 sample show the ordered mesostructure formed in a layer-by-layer fashion (**Figure 2**a). The cross-sectional FESEM image reveals that the uniform mesopores are periodically aligned over a large domain (Figure 2b). Transmission electron microscopy

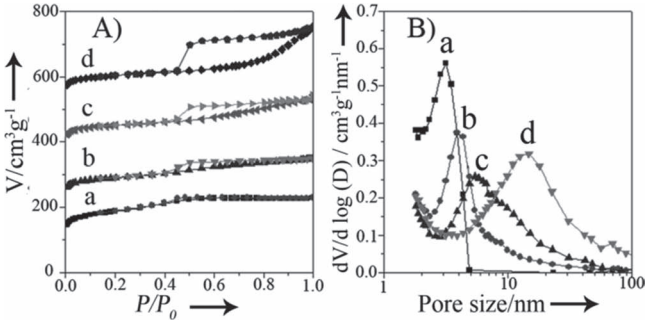

Figure 3. Nitrogen sorption isotherms (A) and pore size distributions (B) of the N-doped mesoporous carbons with different mass ratios of DCDA to resol: a) H-NMC-0; b) H-NMC-1.0; c) H-NMC-1.5; and d) H-NMC-2.5. For clarity, the isotherms curves in (A) are offset by 150 $cm^3\ g^{-1}$ for H-NMC-1.0, 300 $cm^3\ g^{-1}$ for H-NMC-1.5, and 450 $cm^3\ g^{-1}$ for H-NMC-2.5.

(TEM) images and corresponding fast Fourier diffractograms (Figure 2c,d) indicate that the H-NMC-1.5 sample has a high degree of periodicity viewed from [110] and [001] directions, respectively. It further confirms that the H-NMC-1.5 sample has a 2D hexagonal mesostructure (*p6m*). The H-NMC-2.5 sample prepared by using a higher DCDA addition has a degenerated mesostructure with the tubular pores randomly percolated by large pores (Figure 2e). The TEM image further reveals that the alignment of mesopore channels is distorted and decorated by large pores (Figure 2f and inset), which coincides with the SAXS results (Figure 1d).

Nitrogen adsorption–desorption isotherms of the sample H-NMC-0 without adding DCDA (**Figure 3**A, series a) show type-IV curves with a sharp capillary condensation step in the relative pressure range of 0.4–0.6 and H_1-type hysteresis loop, indicative of uniform cylindrical pores. As the mass ratio of DCDA to resol increases to 1.0, 1.5, and then 2.5, the capillary condensation step shifts to high relative pressure ranges, indicating that the pore size increases gradually (Figure 3A, series b to d). The pore size distributions derived from the adsorption branches by using BJH model indicate that, as x increases from 0 to 2.5, the pore size dramatically increases from 3.1 to 14.8 nm (Figure 3B and Table S1 in the Supporting Information). The BET surface area and pore volume of all the N-doped mesoporous carbons are in the ranges 494–658 $m^2\ g^{-1}$ and 0.31–0.47 $cm^3\ g^{-1}$, respectively (Table S1).

By using a higher mass ratio of resol to F127 (2:1), N-doped ordered mesoporous carbons with cubic mesostructure (denoted as C-NMC-x) can be also synthesized via the same synthesis procedure. Similarly, a series of C-NMC-x samples can be obtained by tuning the mass ratio of DCDA to resol in the range 0–2.0. SAXS patterns of C-NMC-0 show three well-resolved peaks which can be indexed to the 110, 200, and 211 planes of a cubic mesostructure with space group of $Im\bar{3}m$ (**Figure 4**). As the DCDA addition amount increases from 0 to 1.5, all the obtained samples display well-resolved 110 peak in their SAXS patterns, indicating that the ordered mesostructures can be well retained in this range. On adding too much DCDA, with x larger than 2.0, the 110 peaks become less resolved, as indicated by the SAXS patterns of C-NMC-2.0 (Figure 4f). The pore size, surface area and pore volume of C-NMC

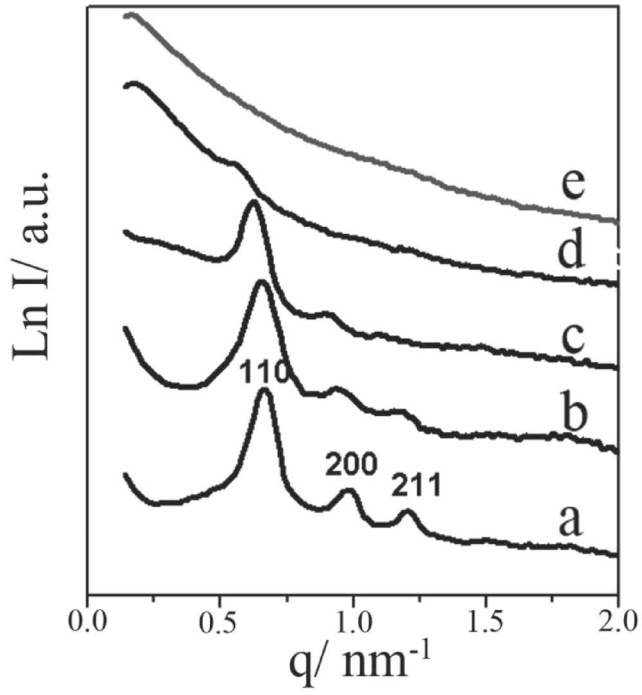

Figure 4. SAXS patterns of the N-doped mesoporous carbon with body-centered-cubic mesostructure prepared from one-pot assembly method by using dicyandiamide as a nitrogen source: a) C-NMC-0; b) C-NMC-0.4; c) C-NMC-0.8; d) C-NMC-1.5; and e) C-NMC-2.0.

samples are in the ranges 3.9–17.6 nm, 500–548 $m^2\ g^{-1}$, and 0.27–0.47 $cm^3\ g^{-1}$, respectively (Figure S1 and Table S1 in the Supporting Information). TEM images of C-NMC-0.8 viewed from the [100], [110], and [111] directions, respectively, further confirm that the obtained materials have highly ordered mesostructures with $Im\bar{3}m$ symmetry (Figure S2a–c in the Supporting Information).[5c] By contrast, the sample C-NMC-2.0 (Figure S2d) obtained with higher mass ratio of DCDA to resol (x = 2.0) reveals lots of randomly distributed large mesopores in the cubic mesoporous carbon matrix, which are probably formed by the decomposition of the excess DCDA. This phenomenon is also observed in the H-NMC-2.5 sample.

Elemental analyses were carried out to measure the chemical composition of N-doped mesoporous carbons (Table S1 in the Suppporting Information). The N content for the series of H-NMC-x samples increases dramatically from 0.089 to 13.1 wt% as the mass ratio of the DCDA to resol increases from 0 to 2.5. Similarly, the C-NMC-x samples with cubic mesostructure show the same trends and their N content increases from 0.086 to 13.74 wt% as the mass ratio of DCDA to resol increases from 0 to 2.0 (Table S1). The X-ray photoelectron spectroscopy (XPS) technique was used to investigate the nature of the nitrogen species in the surface of the N-doped mesoporous carbons. The XPS spectrum of the N-doped mesoporous carbon (H-NMC-2.5) shows strong signals from carbon, nitrogen and oxygen elements (**Figure 5**a). The content of nitrogen is about 10.7 wt%, close to the elemental analysis result (13.10 wt%). This implies that the N element is distributed homogeneously in the framework of ordered mesoporous carbons. Four peaks were observed in N_{1s} spectrum (Figure 5b). The peaks centered at 400.2, 401.2, 402.1, and 403.0 eV are attributed to tertiary nitrogen (N-1), amino functions (C–NH_2; N-2), quaternary nitrogen (N-3), and pyridine-N-oxide (N-4); the contents of the four types of nitrogen atoms are listed in the Figure 5c. This suggests that the basic N atoms (N-1 and N-2) account for up to 60.3% of the content.

On the basis of the above observations, the successful synthesis of N-doped mesoporous carbons with high N content is mainly due to the multi-component co-assembly of DCDA (the nitrogen source), Pluronic F127 (the template molecule) and resol (the carbon source), as depicted in Scheme 1. F127 copolymers have long hydrophilic PEO segments with abundant EO repeating units, which can interact with the phenolic hydroxyl groups of resol molecules via hydrogen bonding. Meanwhile, the H^+ ions from the phenolic hydroxyl groups can be captured by the amine groups of DCDA molecules, resulting in electrostatic interactions between the partly negatively charged resol and positively charged DCDA molecules, which helps to prevent the phase separation of the carbon and nitrogen precursors during the EISA process. During the evaporation of the solvent, with a proper ratio of template molecules and organic precursor, the F127 templates associated with organic resol and DCDA molecules assemble into rod-like composite micelles with hydrophobic PPO segments as the cores of rods surrounded by PEO-resol-DCDA composite shell (Step 1). As the solvent further evaporates, ordered mesostructure can be

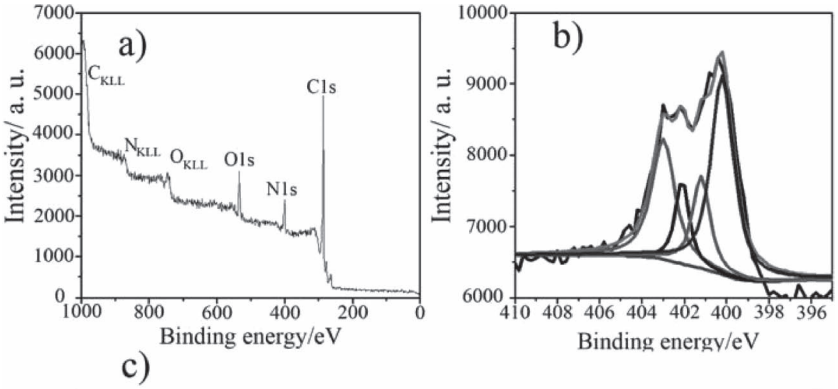

sample	N-1 (%)	N-2 (%)	N-3 (%)	N-4 (%)
	400.2 eV	401.2 eV	402.1 eV	403eV
NMC	44.2	16.1	11.8	27.9

Figure 5. XPS spectra of the N-doped mesoporous carbon with the mass ratio of 2.5 (DCDA/resol) (H-NMC-2.5): a) survey spectrum; b) N_{1s} spectrum; c) is N_{1s} core level peak analyses. Each peak corresponds to a specific type of nitrogen: N-1: tertiary nitrogen, N-2: amino functions (C–NH_2), N-3: quaternary nitrogen, and N-4: pyridine-N-oxide.

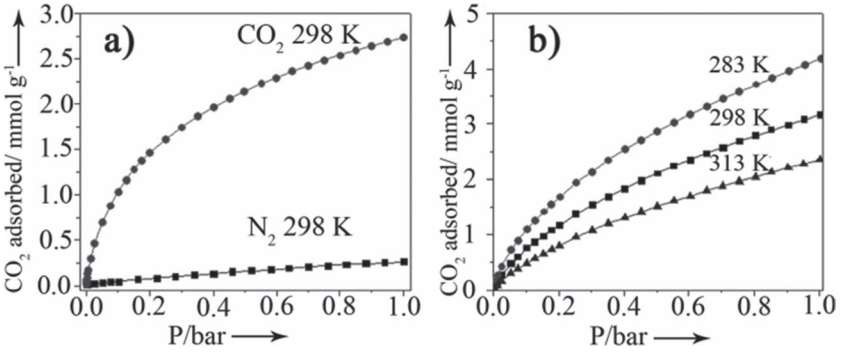

Figure 6. a) CO_2 and N_2 adsorption isotherms at 298 K for the N-doped mesoporous carbon H-NMC-2.5. b) CO_2 adsorption isotherms at different temperature for A-NMC after activation by KOH.

formed via the packing of the rod-like micelles. After heating at 100 °C in air for 24 h, the ordered mesostructure can be fixed by the thermopolymerization of resols, and the DCDA species can be retained in the matrix of phenolic resin (Step 2). The final step of pyrolysis at 600 °C in N_2 can remove the F127 template and carbonize the polymer framework (Step 3). The N contents can be readily adjusted by simply changing the mass ratio of DCDA to resol; a higher ratio leads to higher N content. When the ratio is as high as 2.5, the excess DCDA cannot be well-dispersed in the resol matrix but aggregates into nanoparticles, which further polymerize into melamine particles during pyrolysis. The melamine can sublimate partially at about 325 °C, as revealed by the thermogravimetric analyses and differential scanning calorimeter (DSC) measurements (Figure S3 in the Supporting Information). As a result of the inhomogenous distribution and sublimation of DCDA-derived melamine nanoparticles in the resol matrix, the H-NMC-*x* samples with greater amounts of DCDA have larger mesopore sizes, and broader pore size distribution (Figure 3B, c,d). The formation of C-NMC-*x* materials follows the same process.

The capture of CO_2 has attracted considerable attention in recent years because it is the main anthropogenic contributor to climate change. The CO_2 sorption isotherms of the N-doped mesoporous carbon (H-NMC-2.5) with large surface area (537 m^2 g^{-1}) and high nitrogen content (13.10 wt%) show a high capacity of 2.8 mmol g^{-1} at 298 K and 1.0 bar. By contrast, commercial activated carbons only show CO_2 capacities of 2.1–2.5 mmol g^{-1} at 298 K and 1.0 bar, though they usually have a high surface area of 2000–3000 m^2 g^{-1} (**Figure 6**a).[10] Comparatively, the adsorption capacity of the sample H-NMC-2.5 for N_2 at 298 K and 1.0 bar is only 0.26 mmol g^{-1}. The initial slopes of the CO_2 and N_2 adsorption isotherms are calculated to be 13.59 and 0.37, respectively. Therefore, the ratio of initial slopes is as high as 37:1, indicating that the H-NMC-2.5 has high selectivity in adsorbing CO_2/N_2 mixed gas. To further increase the absorption capacity, the H-NMC-2.5 was activated by KOH at 600 °C for 1 h. After activation, the H-NMC-2.5 shows higher surface area of 1417 m^2 g^{-1} and N content of 6.7 wt% (Table S1 in the Supporting Information). The CO_2 uptake curves indicate an enhanced CO_2 capacity of 3.2 mmol g^{-1} at 298 K and 1.0 bar (Figure 6b). This implies that, with increasing surface area of H-NMC-*x* samples, more active surface with exposed basic sites can significantly improve the CO_2 capacity.[11] Comparatively, the CO_2 capacities at 1.0 bar were measured to be 4.2 and 2.2 mmol g^{-1} at 283 and 313 K, respectively. The higher temperature leads to lower CO_2 adsorption capacity, indicating that the CO_2 adsorption process on the H-NMC-*x* is an exothermic process. To determine the strength of the interaction between CO_2 molecular and activated H-NMC-2.5, the isosteric heat of CO_2 adsorption was calculated using CO_2 adsorption isotherms at 283 and 298 K based on the Clausius-Clapeyron equation. The isosteric heat of adsorption decreases from 38 to 24 kJ mol^{-1} as the CO_2 adsorption amount increases from 0.1 to 3.2 mmol g^{-1} (Figure S4 in the Supporting Information). The high isosteric heat of adsorption is mainly due to

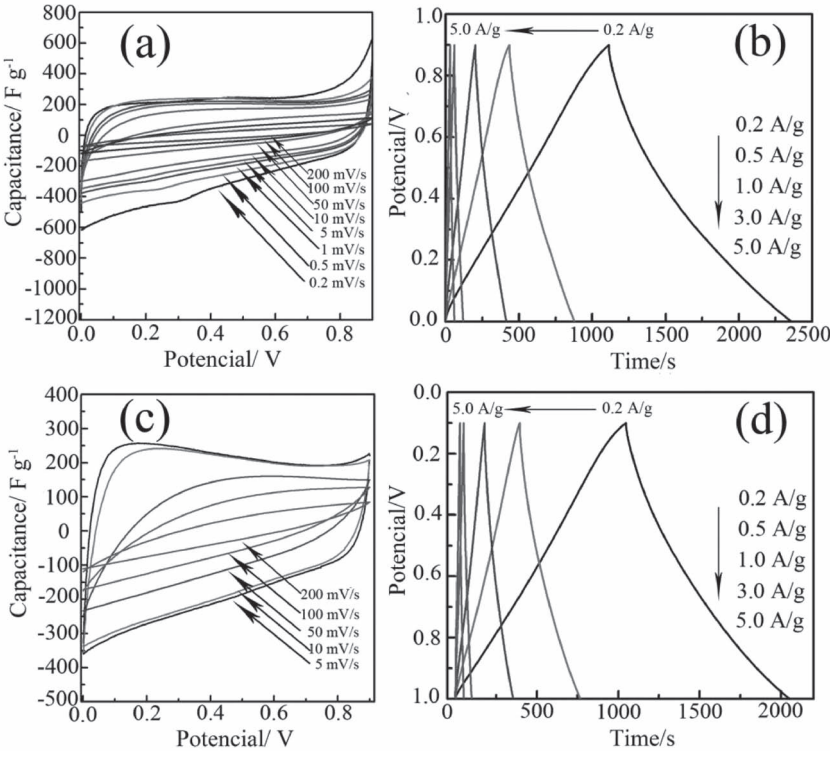

Figure 7. Electrochemical performance of the sample H-NMC-2.5 using a three-electrode cell: cyclic voltammograms at different scan rates in 1 M H_2SO_4 (a) and 6 M KOH (c); and galvanostatic charge/discharge curves at different current densities in 1 M H_2SO_4 (b) and 6 M KOH (d).

the N-containing groups that serve as Lewis bases and readily interact with the acidic CO_2 molecules.

Mesoporous carbon has been widely applied for electrode materials in supercapacitors. The modification of carbon materials with nitrogen functionalities is one of the most promising method to enhance the capacity while maintaining the superb cycleability of the supercapacitor.[3b,c] Herein, inspired by their high surface area and high N content, H-NMC-2.5 was used as the electrode of the supercapacitor. The cyclic voltammetry for H-NMC-2.5 sample in both acidic (1 M H_2SO_4) and basic (6 M KOH) media shows a nearly rectangular shape, suggesting a double-layer capacitance behavior (**Figure 7**). The rectangular shape is retained well even at high scan rate (200 mV s^{-1}). The charge–discharge tests of H-NMC-2.5 sample were conducted at current densities from 0.2 to 5.0 A g^{-1}. The specific capacitances calculated from the charge–discharge curve are ca. 262 F g^{-1} (in H_2SO_4) and 227 F g^{-1} (in KOH) at a current density of 0.2 A g^{-1}. The specific capacitances are 244 F g^{-1} (in H_2SO_4) and 213 F g^{-1} (in KOH) at a current density of 0.5 A g^{-1}, which are much better than that for the mesoporous carbon FDU-15 without N modification (110–130 F g^{-1}).[6b] When the current density increases to 5 A g^{-1}, the specific capacitances of N-doped mesoporous carbon still retain 63% (in H_2SO_4) and 60% (in KOH), respectively (Figure S5 in the Supporting Information).

3. Conclusions

In summary, we demonstrate a facile and controllable one-pot method to synthesize ordered mesoporous carbon with high surface area and high N content by using soluble resol as a carbon source, dicyandiamide as a nitrogen source, and commercial triblock copolymer F127 as a soft template via solvent evaporation induced self-assembly process. Owing to their multiple phenolic hydroxyl groups, resol molecules can serve as a bridge to connect the template F127 and DCDA molecules via hydrogen bonding and electrostatic interactions, which makes the three components co-assembly into ordered mesostructures during the EISA process. The obtained N-doped ordered mesoporous carbons possess tunable mesostructures (hexagonal $p6m$ and cubic $Im\bar{3}m$ symmetry) and pore size (3.1–17.6 nm), high surface area (494–586 m^2 g^{-1}), and high N content (up to 13.1 wt%) by changing the ratio of F127, resol, and DCDA. As a result of their high surface area and high N content, as well as highly accessible mesopores, the N-doped mesoporous carbons show excellent performance as absorbents for CO_2 capture (2.8–3.2 mmol g^{-1}, 298 K, 1.0 bar) and as supercapacitor electrode with high specific capacitance in both acidic (262 F g^{-1}, 1 M H_2SO_4) and basic (227 F g^{-1}, 6 M KOH) media at a current density of 0.2 A g^{-1}. Therefore, it is believed that these N-doped mesoporous carbons are promising as novel versatile nanomaterials for multi-purpose applications in a range of fields. This synthesis concept is applicable for design of mesoporous carbons doped with other elements by choosing appropriate precursors which can interact with resols, be converted stable intermediate phases in situ, and finally endure pyrolysis at a high temperature.

4. Experimental Section

Synthesis of N-Doped Ordered Mesoporous Carbons: For the typical synthesis of the N-doped mesoporous carbon with 2D hexagonal mesostructure, F127 (1.0 g) and different amounts of DCDA (0 to 2.5 g) were first dissolved in a mixture of ethanol (20 g) and water (10 g). Then, 5.0 g of resol ethanol solution (20 wt%) was added and stirred for 0.5 h. In all these syntheses, the mass ratio F127 to resol was fixed at 1:1. Transparent composite films were obtained by pouring the solution into Petri dishes to evaporate the solvent at 50 °C for 6 h. After further heating in an oven at 100 °C for 24 h for thermosetting, the as-made composites were scrapped and crushed into powders for pyrolysis. The pyrolysis was carried out in a tubular furnace under N_2 atmosphere at 250 °C for 2 h and then 600 °C for 3 h with a ramp rate of 1 °C min^{-1}. The samples were denoted as H-NMC-*x* (hexagonal N-doped mesoporous carbon), where *x* is the mass ratio of DCDA to resol.

In activation with KOH, the H-NMC-2.5 sample was chemically activated by heating the mixture of H-NMC-2.5 and KOH powder (mass ratio of KOH/H-NMC-2.5 was 6:1) under N_2 at 600 °C for 1 h with a ramp rate of 5 °C min^{-1}. The product was first washed with 2 M HCl to remove inorganic salts, and then washed with distilled water until the pH value of the filtrate reached 7.0. Finally, the sample was dried in an oven at 100 °C. The activated N-doped mesoporous carbon was denoted as A-NMC. The synthesis of N-doped mesoporous carbons with cubic mesostructure were similar except that the mass ratio of F127 to resol was 1:2, and the obtained samples were denoted as C-NMC-*x* (cubic N-doped mesoporous carbon), where *x* is the mass ratio of DCDA to resol.

Characterization: Small angle X-ray scattering (SAXS) measurements were taken on a Nanostar U small-angle X-ray scattering system (Bruker, Germany) using Cu Kα radiation (40 kV, 35 mA). The *d*-spacing values were calculated from the formula $d = 2\pi/q$. Nitrogen sorption isotherms were measured at 77 K with a Micromeritics Tristar 3020 analyzer (USA). Before measurements, the samples were degassed in a vacuum at 180 °C for at least 6 h. The Brunauer-Emmett-Teller (BET) method was utilized to calculate the specific surface areas. By using the Barrett-Joyner-Halenda (BJH) model, the pore volumes and pore size distributions were derived from the adsorption branches of isotherms, and the total pore volumes (V) were estimated from the adsorbed amount at a relative pressure P/P_0 of 0.995. Transmission electron microscopy (TEM) experiments were conducted on a JEOL 2011 microscope (Japan) operated at 200 kV. Field-emission scanning electron microscopy (FESEM) images were collected on the Hitachi Model S-4800 field emission scanning electron microscope. The dried samples were directly used for the observation without any treatment. Elemental analyses were done on an Elementar Vario EL III microanalyzer. XPS experiments were carried out on a RBD upgraded PHI-5000C ESCA system (Perkin Elmer) with Mg Kα radiation ($h\nu$ = 1253.6 eV) or Al Kα radiation ($h\nu$ = 1486.6 eV). Binding energies were calibrated by using the containment carbon (C_{1s} = 284.6 eV). The CO_2 adsorption isotherms were measured in a temperature-controlled water bath on IGA gravitometer adsorption apparatus. The samples were degassed at 200 °C for 8 h (increasing rate: 10 °C min^{-1}, outgas rate: 50 mbar min^{-1}).

Electrochemistry Test: For fabrication of a working electrode, a mixture containing active materials (80 wt%), acetylene black (10 wt%), and polytetrafluoroethylene (PTFE; 10 wt%) was well mixed to form a homogeneous slurry. The slurry was then pressed onto a titanium screen that serves as a current collector. The typical mass of active material was about 5 mg cm^{-2}, and the thickness of the electrode membrane about 98 μm (estimated apparent electrode density is about 0.51 g cm^{-3}). The electrochemical experiments were carried out using a three-electrode cell, employing platinum as the counter electrode, a saturated calomel electrode (SCE) (0.2415 V vs. the standard hydrogen electrode) as the reference electrode and 1 M H_2SO_4 (or 6 M KOH) solution as the electrolyte. The cyclic voltammetry (CV) and the galvanostatic charge–discharge (GC) tests were performed using electrochemical analyzer, CHI 605B at ambient conditions.

Supporting Information

Supporting Information is available from the Wiley Online Library or from the author.

Acknowledgements

This work was supported by the NSF of China (20890123, 20821140537, and 21073040), the State Key 973 Program of the PRC (2012CB224805), the Shanghai Leading Academic Discipline Project (B108), the Science & Technology Commission of Shanghai Municipality (08DZ2270500), the Innovation Program of Shanghai Municipal Education Commission (13ZZ004), the Shanghai Rising Star Project of STCSM (12QH1400300), and the Key Subjects Innovative Talents Training Program of Fudan University.

Received: September 24, 2012
Published online: December 7, 2012

[1] a) J. Lee, J. Kim, T. Hyeon, *Adv. Mater.* **2006**, *18*, 2073; b) C. D. Liang, Z. J. Li, S. Dai, *Angew. Chem. Int. Ed.* **2008**, *47*, 2; c) A. H. Lu, W. Schmidt, N. Matoussevitch, H. Bönnemann, B. Spliethoff, B. Tesche, E. Bill, W. Kiefer, F. Schüth, *Angew. Chem. Int. Ed.* **2004**, *43*, 4303; d) T. Ohkubo, J. Miyawaki, K. Kaneko, R. Ryoo, N. A. Seaton, *J. Phys. Chem. B* **2002**, *106*, 6523; e) J. Lee, S. Yoon, T. Hyeon, S. M. Oh, K. B. Kim, *Chem. Commun.* **1999**, 2177; f) X. L. Ji, K. T. Lee, L. F. Nazar, *Nat. Mater.* **2009**, *6*, 500; g) S. H. Joo, S. J. Choi, I. Oh, J. Kwak, Z. Liu, O. Terasaki, R. Ryoo, *Nature* **2001**, *412*, 169; h) K. Ariga, A. Vinu, Q. Ji, O. Ohmori, J. P. Hill, S. Acharya, J. Koike, S. Shiratori, *Angew. Chem. Int. Ed.* **2008**, *47*, 7254.

[2] a) A. Y. Liu, M. L. Cohen, *Science* **1989**, *245*, 841; b) Y. D. Xia, R. Mokaya, *Adv. Mater.* **2004**, *16*, 1553; c) A. Vinu, M. Terrones, D. Golberg, S. Hishita, K. Ariga, T. Mori, *Chem. Mater.* **2005**, *17*, 5887; d) D. Hulicova, J. Yamashita, Y. Soneda, H. Hatori, M. Kodama, *Chem. Mater.* **2005**, *17*, 1241; e) T. Durkic, A. Peric, M. Lausevic, A. Dekanski, O. Neskovic, M. Veljkovic, Z. Lausevic, *Carbon* **1997**, *35*, 1567.

[3] a) G. P. Hao, W. C. Li, A. H. Lu, *J. Mater. Chem.* **2011**, *21*, 6447; b) D. H. Jurcakova, M. Kodama, S. Shiraishi, H. Hatori, Z. H. Zhu, G. Q. Lu, *Adv. Funct. Mater.* **2009**, *19*, 1800; c) T. Kwon, H. Nishihara, H. Itoi, Q. H. Yang, T. Kyotani, *Langmuir* **2009**, *25*, 11961; d) F. Goettmann, A. Fischer, M. Antonietti, A. Thomas. *Angew. Chem. Int. Ed.* **2006**, *45*, 4467; e) X. Jin, V. V. Balasubramanian, S. T. Selvan, D. P. Sawant, M. A. Chari, G. Q. Lu, A. Vinu. *Angew. Chem. Int. Ed.* **2009**, *48*, 7884; f) K. K. R. Datta, B. V. S. Reddy, K. Ariga, A. Vinu, *Angew. Chem. Int. Ed.* **2010**, *49*, 5961; g) Y. Wang, X. C. Wang, M. Antonietti, *Angew. Chem. Int. Ed.* **2012**, *51*, 68; h) Y. Zheng, J. Liu, J. Liang, M. Jaroniec, S. Z. Qiao, *Energy Environ. Sci.* **2012**, *5*, 6717; i) Z. X. Wu. P. A. Webley, D. Y. Zhao, *J. Mater. Chem.* **2012**, *22*, 11379; j) R. L. Liu, D. Q. Wu, X. L. Feng, K. Müllen, *Angew. Chem. Int. Ed.* **2010**, *49*, 2565; k) Y. Zheng, Y. Jiao, J. Chen, J. Liu, J. Liang, A. Du, W. Zhang, Z. Zhu, S. C. Smith, M. Jaroniec, G. Q. Lu, S. Z. Qiao, *J. Am. Chem. Soc.* **2011**, *133*, 20116.

[4] a) A. Vinu, K. Ariga, T. Mori, T. Nakanishi, S. Hishita, D. Golberg, Y. Bando, *Adv. Mater.* **2005**, *17*, 1648; b) N. N. Liu, L. W. Yin, C. X. Wang, L. Y. Zhang, N. Lun, D. Xiang, Y. X. Qi, R. Gao, *Carbon* **2010**, *48*, 3579; c) G. P. Mane, S. N. Talapaneni, C. Anand, S. Varghese, H. Iwai, Q. Ji, K. Ariga, T. Mori, A. Vinu, *Adv. Funct. Mater.* **2012**, *22*, 3596.

[5] a) C. D. Liang, K. L. Hong, G. A. Guiochen, J. W. Mays, S. Dai, *Angew. Chem. Int. Ed.* **2004**, *43*, 5785; b) S. Tanaka, N. Nishiyama, Y. Egashira, K. Ueyama, *Chem. Commun.* **2005**, *16*, 2125; c) Y. Meng, D. Gu, F. Q. Zhang, Y. F. Shi, H. F. Yang, Z. Li, C. Z. Yu, B. Tu, D. Y. Zhao, *Angew. Chem. Int. Ed.* **2005**, *44*, 7053; d) F. Q. Zhang, Y. Meng, D. Gu, Y. Yan, C. Z. Yu, B. Tu, D. Y. Zhao, *J. Am. Chem. Soc.* **2005**, *127*, 13508; e) C. D. Liang, S. Dai, *J. Am. Chem. Soc.* **2006**, *128*, 5316; f) Y. H. Deng, T. Yu, Y. Wan, Y. F. Shi, Y. Meng, D. Gu, L. J. Zhang, Y. Huang, C. Liu, X. J. Wu, D. Y. Zhao, *J. Am. Chem. Soc.* **2007**, *129*, 1690; g) J. Wei, Y. H. Deng, J. Y. Zhang, Z. K. Sun, B. Tu, D. Y. Zhao, *Solid State Sci.* **2011**, *13*, 784.

[6] a) C. F. Xue, B. Tu, D. Y. Zhao, *Nano Res.* **2009**, *2*, 242; b) J. X. Wang, C. F. Xue, Y. Y. Lv, F. Zhang, B. Tu, D. Y. Zhao, *Carbon* **2011**, *49*, 4580.

[7] a) K. Kailasam, Y. S. Jun, P. Katekomol, J. D. Epping, W. H. Hong, A. Thomas, *Chem. Mater.* **2010**, *22*, 428; b) J. P. Yang, Y. P. Zhai, Y. H. Deng, D. Gu, Q. Li, Q. L. Wu, Y. Huang, B. Tu, D. Y. Zhao, *J. Colloid Interface Sci.* **2010**, *342*, 579; c) Y. Wang, X. C. Wang, M. Antonietti, Y. J. Zhang, *ChemSusChem* **2010**, *3*, 435.

[8] G. P. Hao, W. C. Li, Dan Qian, G. H. Wang, W. P. Zhang, T. Zhang, A. Q. Wang, F. Schüth, H. J. Bongard, A. H. Lu, *J. Am. Chem. Soc.* **2011**, *133*, 11378.

[9] a) J. S. Lee, X. Q. Wang, H. M. Luo, G. A. Baker, S. Dai, *J. Am. Chem. Soc.* **2009**, *131*, 4596; b) X. Q. Wang, S. Dai, *Angew. Chem. Int. Ed.* **2010**, *49*, 6664; c) W. Yang, T. P. Fellinger, M. Antonietti, *J. Am. Chem. Soc.* **2011**, *133*, 206; d) J. S. Lee, X. Q. Wang, H. M. Luo, S. Dai, *Adv. Mater.* **2010**, *22*, 1004.

[10] a) E. S. Kikkinides, R. T. Yang, S. H. Cho, *Ind. Eng. Chem. Res.* **1993**, *32*, 2714; b) R. V. Siriwardane, M. S. Shen, E. P. Fisher, J. A. Poston, *Energy Fuels* **2001**, *15*, 279.

[11] a) M. Sevilla, P. V. Vigón, A. B. Fuertes, *Adv. Funct. Mater.* **2011**, *21*, 2781; b) W. Xing, C. Liu, Z. Zhou, L. Zhang, J. Zhou, S. Zhuo, Z. Yan, H. Gao, G. Wang, S. Z. Qiao, *Energy Environ. Sci.* **2012**, *5*, 7323.